DØ Note 6485-conf

Combination of D0 measurements of the mass of the top quark

The D0 Collaboration
http://www-d0.fnal.gov

(Dated: August 3, 2016)

We present a combination of measurements of the mass of the top quark by the D0 experiment in the lepton+jets and dilepton channels. We use all the data collected in Run I (1992–1996) at $\sqrt{s} =$ 1.8 TeV and Run II (2001–2011) of the Tevatron $p\bar{p}$ collider, corresponding to integrated luminosities of 0.1 fb^{-1} and 9.7 fb^{-1}, respectively. The result is: $m_{\rm top} = 174.95 \pm 0.40\,(\rm stat) \pm 0.64\,(\rm syst)$ GeV $= 174.95 \pm 0.75$ GeV.

Result for Summer 2016 conferences

I. INTRODUCTION

The top quark is the heaviest known elementary particle, with a mass approximately twice that of the electroweak vector bosons, and 1.4 that of the more recently discovered Higgs boson [1]. Within the standard model (SM), this large mass arises from a large Yukawa coupling (≈ 0.9) to the Higgs field. Because of this, the top quark plays a significant role in the quantum corrections of electroweak theory, and therefore a precise measurement of the top-quark mass is needed to test the consistency of the SM. The observed values of both the mass of the Higgs boson and the Yukawa coupling of the top quark may play a critical role in the history and stability of the universe (see e.g., Ref. [2]).

The top quark was discovered in 1995 by the CDF and D0 collaborations during Run I of the Fermilab Tevatron $p\bar{p}$ collider at $\sqrt{s} = 1.8$ TeV [3, 4]. Run II (2001–2011) at $\sqrt{s} = 1.96$ TeV provided a factor of ≈ 150 more top-antitop pairs than Run I (1992–1996). Using top-antitop pairs produced in the D0 detector, we have measured the top-quark mass in different decay channels using the full integrated luminosity of Run I ($\int \mathcal{L}\, dt = 0.1$ fb^{-1}) and Run II ($\int \mathcal{L}\, dt = 9.7$ fb^{-1}). This note reports the combination of these direct measurements, which supersedes the previous D0 combination of Winter 2011, which had an uncertainty on the top-quark mass of 1.47 GeV [5]. These measurements are also inputs to the Summer 2016 combination of Tevatron measurements of the top quark [6].

The top-quark mass is a fundamental free parameter of the SM. However, its definition depends on the scheme of theoretical calculations used for the perturbative expansion in quantum chromodynamics (QCD). The inputs to the combination presented in this note are the direct measurements calibrated using Monte Carlo (MC) simulations. Hence, the measured mass corresponds to the MC mass parameter. Due to the presence of long range effects in QCD, the MC mass relation to other mass definitions, such as the pole mass or the mass in the modified minimal subtraction ($\overline{\text{MS}}$) scheme, suffers from ambuguities. The ambiguities between the MC mass and the pole mass are ≈ 1 GeV, and is still subject to debate (see e.g., Ref. [7] and references therein). Note that, we have conducted the extraction of the mass of the top quark from the measured $t\bar{t}$ cross section [8], which provides a measurement of the pole mass [9]. However, due to the ambiguity between MC mass and pole mass, this latter measurement is not part of the combination presented in this document.

II. DECAY CHANNELS AND INPUT MEASUREMENTS

Within the SM, the top quark decays into a W boson and a b quark almost 100% of the time. Different channels arise from the possible decays of the pair of W bosons:

i. The "lepton+jets" channel ($\ell +$ jets) corresponds to events ($\approx 30\%$) where one W boson decays into $q\bar{q}'$ and the other into an electron or a muon and a neutrino. These channels have a moderate yield and a moderate background arising from W+jets production, Z+jets production, or multijet processes.

ii. The "dilepton" channel ($\ell\ell'$) corresponds to events ($\approx 4.5\%$) where both W bosons decay into electrons or muons. These channels are quite pure but have a small yield. The background is mainly due to Z+jets, but also receives small contributions from diboson (WW, WZ, ZZ), W+jets, and multijet production.

iii. The "all jets" channel ($\approx 44\%$) has events in which both W bosons decay to $q\bar{q}'$ that evolve into jets. The yield is high, but the background from multijet production is very large.

iv. "tau channels" ($\approx 22\%$) arise from events in which at least one of the W bosons decays into $\tau\nu_\tau$. As the decays $\tau \to$ hadrons$+\nu_\tau$ are hard to identify, they are not exploited in the following. Nonetheless, the decays $\tau \to \ell\nu_\ell\nu_\tau$ provide additional contributions in the $\ell\ell'$ and $\ell +$ jets channels.

The high mass of the top quark ensures that the decay products have high momenta and large angular separations. Reconstructing and identifying $t\bar{t}$ events requires reconstruction and identification of large transverse-momentum electrons, muons, and jets, and the measurement of the imbalance in transverse momentum in each event. Good momentum resolution is required for all these objects, and the jet energy scale (JES) has also to be known with a good precision. Eventually, identifying the b jets is an effective way of improving the purity of the selections. Often, the uncertainty in the measurement due to the JES uncertainty can be reduced by performing an in situ calibration. This calibration exploits the $W \to q\bar{q}'$ decay, that constrains the mass of the corresponding dijet system to $\approx m_W = 80.4$ GeV.

The input measurements of m_{top} used in this combination are shown in Table I, and consist of measurements performed during Run I and Run II in the $\ell\ell'$ and $\ell +$jets channels. The D0 collaboration has also measured the top-quark mass using the "all jets" channel [10]; however, this measurement is not considered in the combination because its uncertainty is too large. As for Run I [11, 12], two $\ell\ell'$ top mass measurements have been performed in Run II using respectively a neutrino weighting [13] technique and a matrix element method [14]. The former measurement is published and the latter has been accepted for publication in Phys. Rev. D. Both are based on the same data, the full D0 data set, and are therefore correlated. The statistical correlation amounts to 64%, which is estimated using a MC ensemble technique, similar to that used to calibrate the individual measurements [15]. The combination of the Run II dilepton measurements discussed in Ref. [15] is used as input to the present combination. We use the BLUE [16] method to combine the $m_{\rm top}$ measurements, following the same procedure and essentially the same classes of uncertainties as used to compute the Tevatron average of $m_{\rm top}$ [17].

TABLE I: Summary of the input measurements to the D0 combination. We also indicate the method used to extract the mass of the top quark from the data (see the corresponding references for further details).

Period	Channel	$\int \mathcal{L}\, dt(\mathrm{fb}^{-1})$	Method	$m_{\rm top}$ (GeV)	Reference
Run I	$\ell\ell'$	0.1	Combination of matrix weighting and neutrino weighting methods	168.4 ± 12.3 (stat) ± 3.6 (syst)	[11, 12]
Run I	$\ell +$ jets	0.1	Matrix element	180.1 ± 3.6 (stat) ± 3.9 (syst)	[18]
Run II	$\ell\ell'$	9.7	Combination of matrix element and neutrino weighting	173.50 ± 1.31 (stat) ± 0.84 (syst)	[13–15]
Run II	$\ell +$ jets	9.7	Matrix element	174.98 ± 0.41 (stat) ± 0.63 (syst)	[19, 20]

III. UNCERTAINTY CATEGORIES

We employ uncertainty categories similar to those used in the previous Tevatron averages [17, 21]. They are divided into sources of same or similar origin. For example, the Signal modeling (Signal) category discussed below includes uncertainties from different systematic sources that are correlated in the modeling of the simulated signal. In this note we use the naming scheme described in Ref. [17]. The names and symbols used for the systematic uncertainties in past D0 or Tevatron combinations are also provided below in parentheses, for comparison.

In situ light-jet calibration (iJES): That part of the JES uncertainty that originates from in situ calibration procedures and has statistical origin. For the D0 Run II $\ell\ell$ measurement, the uncertainty from transferring the ℓ+jets calibration to the dilepton event topology is included in the Light-jet response (dJES) category described below.

Response to $b/q/g$ jets (aJES): That part of the JES uncertainty that originates from differences in detector response between b-jets and light-quark jets.

Model for b jets (bJES): That part of the JES uncertainty that originates from uncertainties specific to the modeling of b jets, and that is correlated across all measurements. This includes the dependence on semileptonic branching fractions and modeling of b quark fragmentation.

Out-of-cone correction (cJES): That part of the JES uncertainty that originates from modeling of uncertainties correlated across all measurements. It specifically includes the modeling uncertainties associated with light-quark fragmentation and out-of-cone corrections. For Run II measurements, it is included in the Light-jet response (dJES) category.

Light-jet response (dJES): The part of the JES uncertainty that includes calibrations of absolute response (energy dependent), the relative response (η-dependent), and, for Run II, the out-of-cone showering correction.

Lepton modeling (LepPt): The systematic uncertainty arising from uncertainties in the scale and resolution of lepton transverse momentum. This was not considered as a source of systematic uncertainty in Run I.

Signal modeling (Signal): The systematic uncertainty arising from uncertainties in $t\bar{t}$ modeling that are correlated across all measurements. This includes the following sources.

i. The uncertainties associated with initial and final state radiation, and from choice of parton density functions used to generate the $t\bar{t}$ Monte Carlo events for calibrating each method.

ii. The uncertainty from higher-order corrections evaluated from a comparison of $t\bar{t}$ samples generated with MC@NLO [22] and ALPGEN [23], both interfaced to HERWIG [24, 25] for the simulation of parton showers and hadronization.

iii. The systematic uncertainty arising from a change in the phenomenological description of color reconnection (CR) between final state particles [26]. It is obtained from the difference between samples generated using PYTHIA with the Perugia 2011 tune and samples generated using PYTHIA with the Perugia 2011NOCR tune [27]. This uncertainty was not evaluated in Run I since the Monte Carlo generators available at that time did not provide such flexibility in modeling CR. These measurements therefore do not include this source of systematic uncertainty.

iv. The systematic uncertainty associated with the choice of the MC generator used to calibrate the extraction of m_{top}. It includes the changes observed when substituting PYTHIA [28](Run I and Run II) or ISAJET [29] (Run I) for HERWIG [24, 25] when modeling $t\bar{t}$ signal.

Jet modeling (DetMod): The systematic uncertainty arising from uncertainties on jet resolution and identification.

b tag modeling (b-tag): The uncertainty related to the modeling of the b tagging efficiency and the light-quark jet rejection factors in MC simulation relative to data.

Background from theory (BGMC): This systematic uncertainty on the background originating from theory (MC) takes into account the uncertainty in modeling the background sources. It is correlated among all measurements in the same channel, and includes uncertainties on background composition, normalization, and distributions.

Background based on data (BGData): This includes uncertainties associated with the modeling of multijet background in ℓ+jets channels, and multijet and W+jets backgrounds in $\ell\ell$ channels, based on data. This also includes effects of trigger uncertainties which are determined using data.

Calibration method (Method): The systematic uncertainty arising from any source specific to a particular fitting method, including the impact of the finite number of MC events available to calibrate each method.

Offset (UN/MI): This includes the uncertainty arising from uranium noise in the D0 calorimeter and from the corrections to the JES due to multiple interactions. While these uncertainties were sizable in Run I, in Run II, owing to the shorter calorimeter electronics integration time and in situ JES calibration, they are negligible.

Multiple interactions model (MHI): The systematic uncertainty arising from a mismodeling of the distribution of the number of collisions per Tevatron bunch crossing due to the steady increase in instantaneous luminosity during data-taking.

Table II summarizes the different input measurements and their corresponding statistical and systematic uncertainties.

IV. CORRELATIONS

The following correlations are used to combine the measurements:

i. The uncertainties in Statistical uncertainty (Stat) and Calibration method (Method) are taken to be uncorrelated among the measurements.

ii. The uncertainties in the In situ light-jet calibration (iJES) category are taken to be correlated among the Run II measurements since the $\ell\ell'$ measurement uses the JES calibration determined in the ℓ+jets channel.

iii. The uncertainties in Response to $b/q/g$ jets (aJES), Light-jet response (dJES), Lepton modeling (LepPt), b-tag modeling (b-tag), and Multiple interactions model (MHI) are taken to be 100% correlated among the Run I and the Run II measurements but uncorrelated between Run I and Run II.

iv. The uncertainties in the Jet modeling (DetMod) and Offset (UN/MI) categories are taken to be 100% correlated among all measurements.

v. The uncertainties in Backgrounds estimated from theory (BGMC) are taken to be 100% correlated among all measurements in the same channel.

vi. The uncertainties in Backgrounds estimated from data (BGData) are uncorrelated.

vii. The uncertainties in the Model for b jets (bJES), Out-of-cone correction (cJES), and Signal modeling (Signal) are taken to be 100% correlated among all measurements.

A summary of the correlations between the different systematic categories is shown in Table III. Using the inputs from Table II and the correlations specified in Table III, we obtain an overall matrix of correlation coefficients given in Table IV.

TABLE II: Summary of measurements used to determine the D0 average $m_{\rm top}$. Integrated luminosity ($\int \mathcal{L}\ dt$) has units of fb^{-1}, and all other numbers are in GeV. The uncertainty categories and their correlations are described in Section III. The total systematic uncertainty and the total uncertainty are obtained by adding the relevant contributions in quadrature. The symbol "n/a" stands for "not applicable" and the symbol "n/e" for "not evaluated" but expected to be negligible.

	D0 Run I		D0 Run II	
	ℓ+jets	$\ell\ell$	ℓ+jets	$\ell\ell$
$\int \mathcal{L}\ dt$	0.1	0.1	9.7	9.7
$m_{\rm top}$	180.10	168.40	174.98	173.50
In situ light-jet calibration (iJES)	0.00	0.00	0.41	0.47
Response to $b/q/g$ jets (aJES)	0.00	0.00	0.16	0.28
Model for b jets (bJES)	0.71	0.71	0.09	0.13
Out-of-cone correction (cJES)	2.00	2.00	n/a	n/a
Light-jet response (dJES)	2.53	1.12	0.21	0.31
Lepton modeling (LepPt)	n/e	n/e	0.01	0.08
Signal modeling (Signal)	1.10	1.80	0.35	0.43
Jet modeling (DetMod)	0.00	0.00	0.07	0.14
b-tag modeling (b-tag)	0.00	0.00	0.10	0.22
Background from theory (BGMC)	1.00	1.10	0.06	0.00
Background based on data (BGData)	0.00	0.00	0.09	0.08
Calibration method (Method)	0.58	1.14	0.07	0.14
Offset (UN/MI)	1.30	1.30	n/a	n/a
Multiple interactions model (MHI)	n/e	n/e	0.06	0.07
Systematic uncertainty (syst)	3.89	3.63	0.63	0.84
Statistical uncertainty (stat)	3.60	12.30	0.41	1.31
Total uncertainty	5.30	12.83	0.75	1.56

TABLE III: Summary of correlations among sources of uncertainties. The symbols $\times$ or $\otimes$ within any category indicate the uncertainties that are 100% correlated. The uncertainties marked as $\times$ are uncorrelated with those marked as $\otimes$. The symbol 0 indicates absence of correlations. The absence of symbol indicates that the uncertainty is negligible.

	Run I		Run II	
	$\ell+$jets	$\ell\ell'$	$\ell+$jets	$\ell\ell'$
In situ light-jet calibration (iJES)			$\times$	$\times$
Response to $b/q/g$ jets (aJES)	$\otimes$	$\otimes$	$\times$	$\times$
Model for b jets (bJES)	$\times$	$\times$	$\times$	$\times$
Out-of-cone correction (cJES)	$\times$	$\times$	$\times$	$\times$
Light-jet response (dJES)	$\otimes$	$\otimes$	$\times$	$\times$
Lepton modeling (LepPt)	$\otimes$	$\otimes$	$\times$	$\times$
Signal modeling (Signal)	$\times$	$\times$	$\times$	$\times$
Jet modeling(DetMod)	$\times$	$\times$	$\times$	$\times$
b-tag modeling (b-tag)	$\otimes$	$\otimes$	$\times$	$\times$
Background from theory (BGMC)	$\times$	$\otimes$	$\times$	$\otimes$
Background based on data (BGData)	0	0	0	0
Calibration method (Method)	0	0	0	0
Offset (UN/MI)	$\times$	$\times$		
Multiple interactions model (MHI)	$\otimes$	$\otimes$	$\times$	$\times$
Statistical				

TABLE IV: The matrix of correlation coefficients used to determine the Tevatron average top-quark mass.

	Run I, $\ell+$jets	Run I, $\ell\ell'$	Run II, $\ell+$jets	Run II, $\ell\ell'$
Run I, $\ell+$jets	1.00			
Run I, $\ell\ell'$	0.16	1.00		
Run II, $\ell+$jets	0.13	0.07	1.00	
Run II, $\ell\ell'$	0.07	0.04	0.43	1.00

V. RESULTS

The resulting combined value for the top-quark mass is

$$174.95 \pm 0.40\,(\text{stat}) \pm 0.64\,(\text{syst})\ \text{GeV}.$$

Adding the statistical and systematic uncertainties in quadrature yields a total uncertainty of 0.75 GeV, corresponding to a relative precision of 0.43% on the top-quark mass. The combination has a χ^2 of 2.5 for 3 degrees of freedom, corresponding to a probability of 47%, indicating good agreement among all input measurements. The breakdown of the uncertainties is shown in Table V. The total statistical and systematic uncertainties are reduced relative to the published D0–CDF combination [17] due primarily to the latest, most accurate, D0 $\ell+$jets analysis [19, 20].

The pulls and weights for each of the inputs obtained from the combination through the BLUE method, are listed in Table VI. The correlations between the uncertainties cause the weights of the different input channels to differ from what would be expected from the total uncertainty of each measurement reported in Table II.

TABLE V: Combination of D0 measurements of m_{top} and contributions to its overall uncertainty. The uncertainty categories are defined in the text. The total systematic uncertainty and the total uncertainty are obtained by adding the relevant contributions in quadrature.

	D0 combined values (GeV)
m_{top}	174.95
In situ light-jet calibration (iJES)	0.41
Response to $b/q/g$ jets (aJES)	0.16
Model for b jets (bJES)	0.09
Out-of-cone correction (cJES)	0.00
Light-jet response (dJES)	0.21
Lepton modeling (LepPt)	0.01
Signal modeling (Signal)	0.35
Jet modeling (DetMod)	0.07
b-tag modeling (b-tag)	0.10
Background from theory (BGMC)	0.06
Background based on data (BGData)	0.09
Calibration method (Method)	0.07
Offset (UN/MI)	0.00
Multiple interactions model (MHI)	0.06
Systematic uncertainty (syst)	0.64
Statistical uncertainty (stat)	0.40
Total uncertainty	0.75

TABLE VI: The pull and weight for each of the input channels resulting of the BLUE method to determine the average top-quark mass. Numbers are shown with two significant digits.

	D0 Run I		D0 Run II	
	$\ell+$jets	$\ell\ell'$	$\ell+$jets	$\ell\ell'$
Pull	0.98	−0.51	0.63	−1.06
Weight	0.00	−0.00	0.96	0.03

The input measurements and the resulting D0 average mass of the top quark are summarized in Fig. 1, along with the top-quark pole mass extracted by D0 from the measurement of the $t\bar{t}$ cross section [8].

VI. SUMMARY

We have presented the combination of the D0 measurements of the top-quark mass performed with the full data set. Taking into account the statistical and systematic uncertainties and their correlations, the preliminary result for the D0 average is $m_{\text{top}} = 174.95 \pm 0.75$ GeV, where the total uncertainty is obtained assuming Gaussian systematic uncertainties. The measurement of the mass thus has a relative precision of 0.43%. The central value is 0.1 GeV below the previous D0 average obtained in Winter 2011 and 0.6 GeV above the Tevatron average in Summer 2016 [6].

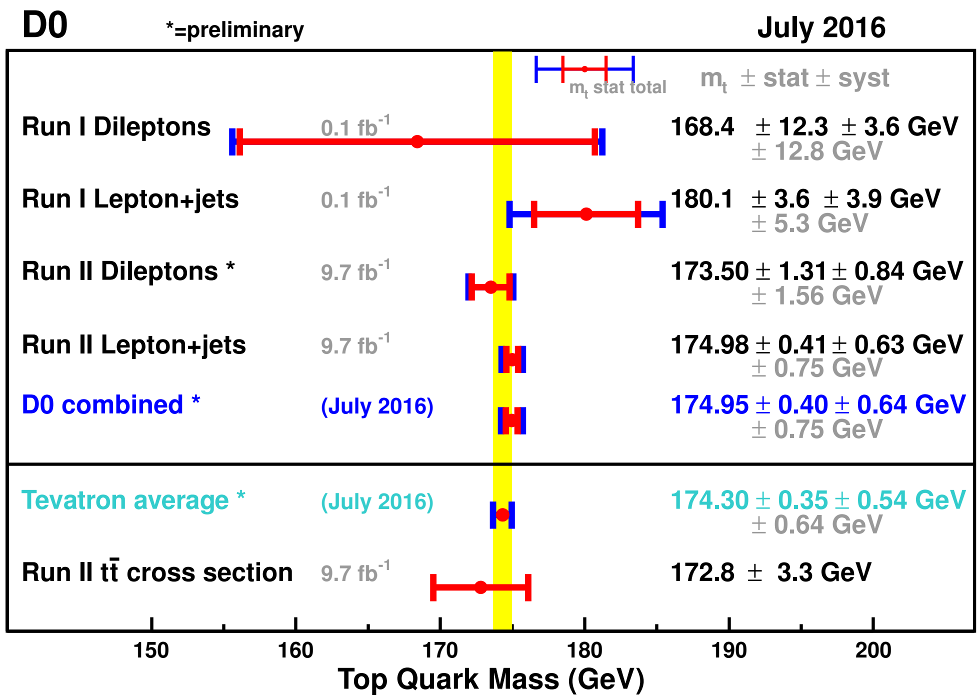

FIG. 1: A summary of the m_{top} measurements used in the D0 combination, along with the D0 combination result, the Tevatron average of m_{top}, and the top-quark pole mass extracted from the cross section measurement. The latter value is not used in the combination.

VII. ACKNOWLEDGMENTS

We thank the staffs at Fermilab and collaborating institutions, and acknowledge support from the DOE and NSF (USA); CEA and CNRS/IN2P3 (France); MON, NRC KI, and RFBR (Russia); CNPq and FAPERJ (Brazil); DAE and DST (India); Colciencias (Colombia); CONACyT (Mexico); NRF (Korea); FOM (The Netherlands); STFC and The Royal Society (UK); MSMT (Czech Republic); BMBF and DFG (Germany); SFI (Ireland); Swedish Research Council (Sweden); CAS and CNSF (China); and MESU (Ukraine).

---

[1] G. Aad *et al.* (ATLAS and CMS Collaborations), Combined Measurement of the Higgs Boson Mass in pp Collisions at $\sqrt{s} = 7$ and 8 TeV with the ATLAS and CMS Experiments, Phys. Rev. Lett. **114**, 191803 (2015).
[2] G. Degrassi, S. Di Vita, J. Elias-Miro, J. R. Espinosa, G. F. Giudice, G. Isidori, and A. Strumia, Higgs mass and vacuum stability in the Standard Model at NNLO, JHEP **08**, 098 (2012).
[3] F. Abe *et al.* (CDF Collaboration), Observation of top quark production in $\bar{p}p$ collisions, Phys. Rev. Lett. **74**, 2626 (1995).
[4] S. Abachi *et al.* (D0 Collaboration), Observation of the top quark, Phys. Rev. Lett. **74**, 2632 (1995).
[5] V. M. Abazov *et al.* (D0 Collaboration), Combination of the D0 top quark mass measurements (2011), D0 Note 5745-CONF.
[6] Tevatron Electroweak Working Group (CDF and D0 Collaborations), Combination of CDF and D0 results on the mass of the top quark using up to 9.7 fb^{-1} at the Tevatron (2016), arXiv:1608.01881.
[7] A. Juste, S. Mantry, A. Mitov, A. Penin, P. Skands, E. Varnes, M. Vos, and S. Wimpenny, Determination of the top quark mass circa 2013: methods, subtleties, perspectives, Eur. Phys. J. **C74**, 3119 (2014).
[8] V. M. Abazov *et al.* (D0 Collaboration), Measurement of the inclusive $t\bar{t}$ production cross section in $p\bar{p}$ collisions at $\sqrt{s} = 1.96$ TeV and determination of the top quark pole mass, Accepted by Phys. Rev. D (2016).

[9] U. Langenfeld, S. Moch, and P. Uwer, Measuring the running top-quark mass, Phys. Rev. D **80**, 054009 (2009).
[10] V. M. Abazov *et al.* (D0 Collaboration), Measurement of the top quark mass in all-jet events, Phys. Lett. B **606**, 25 (2005).
[11] B. Abbott *et al.* (D0 Collaboration), Measurement of the top quark mass using dilepton events, Phys. Rev. Lett. **80**, 2063 (1998).
[12] B. Abbott *et al.* (D0 Collaboration), Measurement of the top quark mass in the dilepton channel, Phys. Rev. **D60**, 052001 (1999).
[13] V. M. Abazov *et al.* (D0 Collaboration), Precise measurement of the top quark mass in dilepton decays using optimized neutrino weighting, Phys. Lett. B **752**, 18 (2016).
[14] V. M. Abazov *et al.* (D0 Collaboration), Measurement of the Top Quark Mass Using the Matrix Element Technique in Dilepton Final States, Submitted to: Phys. Rev. D (2016).
[15] V. M. Abazov *et al.* (D0 Collaboration), Combination of the matrix element and neutrino weighting measurements of the top quark mass in dilepton final states (2016), D0 Note 6484-CONF.
[16] A. Valassi, Combining correlated measurements of several different physical quantities, Nucl. Instrum. Methods Phys. Res., Sect. A **500**, 391 (2003).
[17] T. Aaltonen *et al.* (CDF and D0 Collaborations), Combination of the top-quark mass measurements from the Tevatron collider, Phys. Rev. D **86**, 092003 (2012).
[18] V. M. Abazov *et al.* (D0 Collaboration), A precision measurement of the mass of the top quark, Nature **429**, 638 (2004).
[19] V. M. Abazov *et al.* (D0 Collaboration), Precision measurement of the top-quark mass in lepton+jets final states, Phys. Rev. Lett. **113**, 032002 (2014).
[20] V. M. Abazov *et al.* (D0 Collaboration), Precision measurement of the top-quark mass in lepton+jets final states, Phys. Rev. D **91**, 112003 (2015).
[21] Tevatron Electroweak Working Group (CDF and D0 Collaborations), Combination of CDF and D0 results on the mass of the top quark using up to 9.7 fb^{-1} at the Tevatron (2014), arXiv:1407.2682.
[22] S. Frixione and B. R. Webber, Matching NLO QCD computations and parton shower simulations, J. High Energy Phys. **06**, 029 (2002).
[23] M. L. Mangano, F. Piccinini, A. D. Polosa, M. Moretti, and R. Pittau, ALPGEN, a generator for hard multiparton processes in hadronic collisions, J. High Energy Phys. **07**, 001 (2003).
[24] G. Marchesini, B. R. Webber, G. Abbiendi, I. G. Knowles, M. H. Seymour, and L. Stanco, HERWIG: A Monte Carlo event generator for simulating hadron emission reactions with interfering gluons. Version 5.1 - April 1991, Comput. Phys. Commun. **67**, 465 (1992).
[25] G. Corcella *et al.*, HERWIG 6.5: an event generator for hadron emission reactions with interfering gluons (including supersymmetric processes), J. High Energy Phys. **01**, 010 (2001).
[26] P. Z. Skands and D. Wicke, Non-perturbative QCD effects and the top mass at the Tevatron, Eur. Phys. J. **C52**, 133 (2007).
[27] P. Z. Skands, Tuning Monte Carlo Generators: The Perugia Tunes, Phys. Rev. D **82**, 074018 (2010).
[28] T. Sjostrand, S. Mrenna, and P. Z. Skands, PYTHIA 6.4 physics and manual, J. High Energy Phys. **05**, 026 (2006).
[29] F. E. Paige and S. D. Protopopescu, BNL Reports 38034 and 38774 (1986). (unpublished).